

ADAPTIVE POLE-ZERO CANCELLATION IN GRINDING FORCE CONTROL

PART II: CONTROLLER DEVELOPMENT AND IMPLEMENTATION

Hodge E. Jenkins¹

Georgia Institute of Technology
The George W. Woodruff School
of Mechanical Engineering
Atlanta, GA 30332-0405

Thomas R. Kurfess

Georgia Institute of Technology
The George W. Woodruff School
of Mechanical Engineering
Atlanta, GA 30332-0405

ABSTRACT

This is the second part of a two-part series on the development of an adaptive force controller for the grinding process. Part I developed the basis for a real-time grinding model and revealed the variable nature of the grinding process. This paper uses that real-time grinding model to determine and implement an adaptive control strategy for stable force regulation by reduction of the grinding process variation. Specifically an adaptive pole-zero cancellation technique is investigated to cancel the grinding process variation. Real-time estimation and controller designs are implemented using parallel processors for higher speed control capability than is presently available in machine tool controllers.

The results of this research have culminated in a stable adaptive force controller for the grinding process. This approach to grinding force control has demonstrated the potential for increasing productivity with the reduction of tary time in plunge grinding, showing higher force regulation fidelity than conventional fixed-gain controllers. The implementation of this adaptive pole-zero cancellation approach in surface (traverse) grinding provides a superior surface following capability for fine finishing, as compared to fixed gain controllers.

BACKGROUND

Generally fixed-gain controllers (such as PID-type controllers) are preferred for applications because of their simplicity in implementation. These controllers are easily tuned using simple approaches. However, many processes or systems vary sufficiently to limit the usefulness or stability of fixed-gain controllers. In these cases adaptive control may be applied to maintain stability and improve performance. Grinding has been shown to be a time varying process that can benefit from the application of such a controller.

¹ Author is presently with Lucent Technologies in Norcross, GA.

In this research an adaptive force controller with a real-time process estimator is developed. The desired objective of this research is to provide a methodology for a stable force control in grinding to reduce tary time and maintaining geometry in fine finishing, despite grinding process variation.

Traditionally the control of a machine tool, such as a grinder, consists of servoing the tool position and feed velocity. However, the process forces, applied power, and the material removal rate during grinding must also be considered to effectively produce parts without damage. Another consideration is that grinding is a noisy and time-varying process that is affected by changing properties and conditions in the grinding wheel, material, and existing surface profile.

As shown in Part I, a real-time model of the process is needed to accurately represent the grinding process sufficiently to provide better control. This paper describes in detail the controller designs for the experimental grinding system. A fixed-gain force controller is used for comparison with the adaptive controller in the benchmark experiments to assess performance improvement. The adaptive controller uses pole-zero cancellation and direct design methods to be self-tuning. The design approach and stability evaluation of the adaptive force controller, based on the previously described real-time process model, is presented.

Adaptive Controllers

Adaptive controllers can be divided into two basic types, direct and indirect methods (Astrom, 1986). Direct and indirect refers to the updated controller gains. A common representative of a direct adaptive controller is the model reference adaptive controller (MRAC). Here a model is used to tune the system gains to perform like the model. In general, the MRAC updates the controller parameters directly, (no intermediate calculations are required).

The self-tuning regulator (STR) is an indirect method, as a design procedure is used to determine controllers parameters. The STR uses model parameter estimation to determine current states for use in the real-time design calculations to adjust the controller parameters. The widely used explicit MRAC scheme of Landau (1979) for discrete SISO plants is based on the perfect cancellation of stable plant poles with controller zeros. In this research the STR is the approach taken. The estimated grinding process model is used to update the controller design and subsequently select new gains, providing a fast and robust system.

It should be noted that the use of MRAC and other adaptive methods have been successfully applied in milling and turning. However, the limitations of these systems involve the speed the

servo update of the complete system with a force loop. Indeed, servo update rates for adaptive control have been low. For example Kolarits (1990) had a servo update rate of only 9 Hz and Fussell (1988) had 8 Hz update, both for adaptive force control for end milling. The hardware speeds and the parallel processor design of the control and estimation architecture (presented in the discussion of experimental apparatus in Part I) permit a force control loop with a servo rate of 450 Hz. This faster force servo loop update rate should yield better force regulation, than those of previous efforts.

CONTROLLER DESIGN

The force controllers designed in this research are implemented on a programmable multi-axis controller (PMAC) as described in Part I. The force control is accomplished by an outer force loop and an inner position loop. A block diagram of the overall system is depicted in Figure 1. The system model consists of several functional blocks: force controller, $G_{FC}(s)$, the PMAC position control loop, $G_{PC}(s)$, the tool-workpiece process interaction, $G_{TWP}(s)$, as well as the estimation and adaptation functions. The gains of the adaptive force controller are updated in real-time from the host computer that estimates the grinding process parameters and determines the force controller gains accordingly.

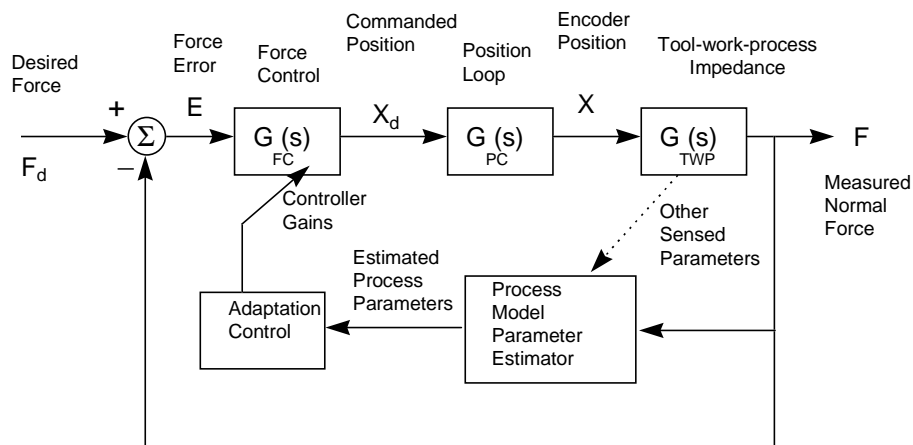


Figure 1. Plant and Controller Schematic for PMAC-based Force Control.

Controller Specifications

It is the goal of this research to develop an adaptive force controller that will provide increased normal force regulation bandwidth by addressing grinding process variations. Thus, it is desired that the adaptive system improve on the actual performance of a fixed-gain force controller designed to the specifications outlined. It should be noted that force regulation is not always desirable for grinding. If the geometry of the part is not near net shape with high spots, force regulation will not remove these unwanted high spots.

Steady State Error

Normal forces have been shown to vary during a typical grinding, attributable to the varying nature of the grinding. To ensure the repeatability of machine deflections, ground part dimension, and to prevent wheel damage, it is desired to grind at a constant, pre-determined force level. Thus, it is desired that the grinding system have a zero steady-state error to a step command in the desired force.

It is also desired to have no steady-state displacement error for the displacement plunge grinding experiments with step commands in position. The desired position must be obtained for dimensional accuracy.

Percent Overshoot

Trajectory overshoot is a major concern in grinding. If the system overshoots the desired force level, surface damage, sub-surface damage, or thermal damage may occur to the work piece or to the grinding wheel. Position overshoots can remove more material than desired, creating dimensional errors or be amplified by the tool-workpiece impedance to create excess forces. The desired performance of the closed-loop system for no overshoot would be that of first order system or a second order system with an damping ratio of more than 0.707 (but less than critically damped).

Rise Time

The 95% rise time is desired to be low as possible to provide quick changes in force without significant delays. Expectation for rise time is under a quarter of a second for the force loop;

however, it is important to verify that the design parameters are chosen to meet the target. It should be noted that since the position loop is an inner loop, to the overall controller, its rise time (and bandwidth) must be significantly faster to achieve the desired force rise time.

Gain Plots

Another set of tools applied to the controller designs are gain plots. Gain plots show the explicit variation of the roots of the plant characteristic equation. The closed-loop pole magnitudes and angles are plotted versus a key scalar parameter of interest, such as the forward loop gain (Kurfess and Nagurka, 1994). An advantage of the gain plots is that the pole locations are depicted as explicit functions of gain or a parameter of interest.

CONTROLLER DESIGN

The controllers are synthesized using the model of the system and process developed in Part I and using control design tools that address classical design, digital design, and robustness issues. Since force is being controlled via position, two control loops must be designed, a position loop and a force loop.

The servo controller for the position loop is implemented using the resident PID-type (proportional, integral and derivative) servo algorithm in the PMAC. The PC-based PMAC controller software interface provides a tuning utility to determine the position loop gains for a desired bandwidth and damping ratio. These are based on the Ziegler-Nichols (Franklin 1992) PID tuning techniques. This tuning utility is used to determine the PID algorithm gains for position control response during normal axis movement operations (while not engaged in force control). The system has a natural integrator in the position loop, but integral control is necessary to overcome the servo stage friction and variable external loads in the discrete implementation. Although integral control is used to eliminate the possibility of steady state position errors, it is not desired when the position loop is nested in the force loop, as position integration can lead to an oscillatory force behavior.

FORCE CONTROLLER

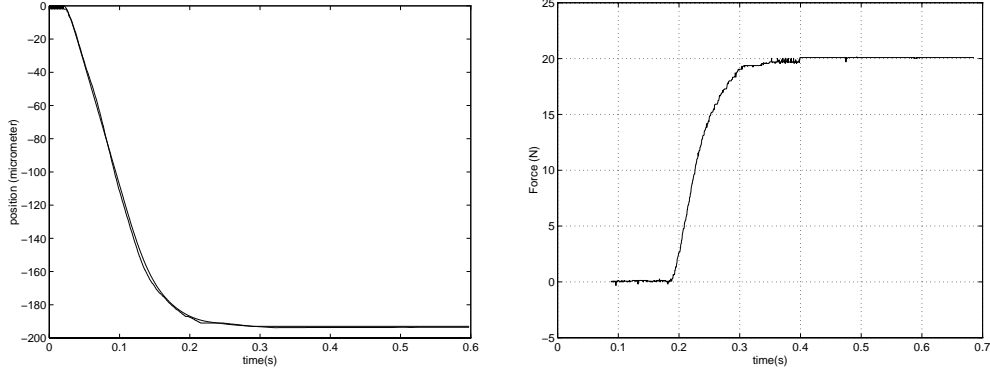
A block diagram of the complete grinding system and controller without the estimation and adaptive control elements is shown in Figure 1. In this case the grinding system model consists of several functional blocks, (1) force controller, $G_{FC}(s)$, (2) PMAC position control loop, $G_{PC}(s)$, (3) the grinding wheel to workpiece and process interaction, $G_{TWP}(s)$. The force sensor response is approximately unity over the frequency range of interest (0-20 Hz), from the calibration data.

The force controller is implemented as a motion program on the PMAC, running continuously. The effective sampling rate is dependent on the number of calculations in the program. The position loop has priority because it is a service interrupt, therefore, the force controller is always slower. The measured force sampling rate is 5-servo cycles.

The PMAC position loop transfer function, $G_{PC}(s)$, is represented by block between the commanded position and the actual position of the X-axis, as measured by the encoder. Because the servo loop for position is very fast (0.445 ms update) a linear, first order model of the position loop servo response, $G_{PC}(s)$, is estimated using an auto-regressive, least squares parameter estimation technique. This is accomplished by performing several force servo experiments with the grinding wheel in contact with the workpiece. It is important to obtain the position model at the anticipated force levels to determine the correct position response, including the imposed force.

The identified model and experimental data are in agreement as can be seen by Figure 2, that (a correlation coefficient of 0.999 was found). The resulting frequency domain transfer function between the commanded position (x_d) and the actual position (x_e) of the grinder X-axis is given in equation (1). Although the transfer function from the applied motor voltage to the resulting shaft angle generally implies a second order model, a first order plant model is found adequate for the system.

$$G_{PC}(s) = \frac{X_e(s)}{X_d(s)} = \frac{203}{s + 224} \quad (1)$$



(a) Axial Displacement and ARX

(b) Corresponding Measured Force

Figure 2. Model Response to Commanded Input.

Fixed-Gain Force Control Design

For the initial experiments and for comparison to the adaptive force controller a fixed-gain force controller is designed ignoring the grinding process dynamics. The tool-workpiece process interaction, $G_{TWP}(s)$, is approximated as a spring, K_s . Thus, a simplified representation of the plant and tool-workpiece interaction can be thought of as a first order system of Type 0.

$$G_{PC}(s)G_{TWP}(S) = \frac{F(s)}{X_D(s)} = \frac{203K_s}{s + 224} \quad (2)$$

To eliminate the steady-state force error from a step command in force a proportional integral (PI) type controller is selected for the force control of the grinding system. The continuous representation of the force controller transfer function, $G_{FC}(s)$, is given in equation (3).

$$G_{FC}(s) = K_{PROP} \left(s + \frac{K_I}{K_{PROP}} \right) \frac{1}{s} \quad (3)$$

The combined plant and controller transfer function in the continuous domain is given in equation (4)

$$G_{FC}(s)G_{PC}(s)G_{TWP}(S) = \frac{F(s)}{E_F(s)} = \frac{203K_s K_{PROP} (s + K_I/K_{PROP})}{s(s + 224)} \quad (4)$$

Thus the overall system gain can be defined as K_F .

$$K_F = 203K_S K_{PROP} \quad (5)$$

It can be seen from equation (2), that the combined system is Type I and will automatically satisfy the zero steady-state error requirement for a step input. From a frequency domain perspective it is desirable to have a high ratio of integral to proportional gain, placing the transmission zero farther along the negative real axis. Since a non-oscillatory force response is also desired, the upper bound to the ratio of integral to proportional gain is the magnitude of the system pole. Larger values of this ratio will cause the system roots to move away from the real axis as the proportional gain is increased. This can be seen in the root locus plots of Figure 3. Considerations for determining the ratio of the integral gain to the proportional gain include the amount of force overshoot for step changes, the rise time of the force regulation, as well as actuator saturation. In the case of the controller zero at $s > -224$, the roots are real for all values of proportional gain. For the case where the controller zero is at $s < -224$, there are break points and the potential for an oscillatory response. As there is always some uncertainty in the estimation of the identified plant, it is desirable to have the controller zero away from the system pole at $s = -250$.

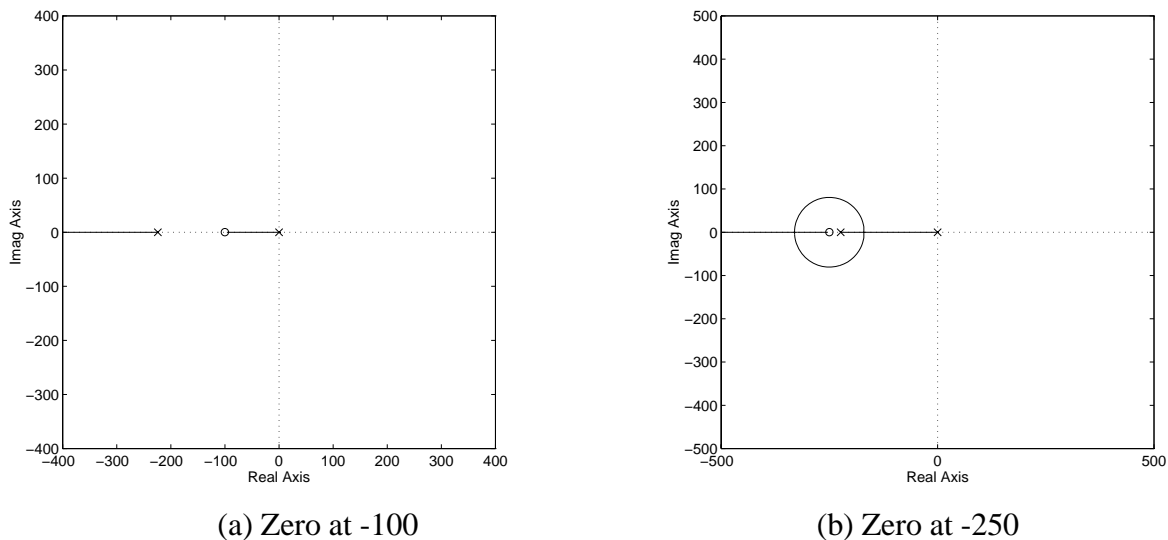


Figure 3. Root Locus Plots for Various Zero Placements.

As is seen in both the root locus and gain plots, the system poles begin on the real axis and can break out when the zero is farther to left of the fastest pole (zero at $s < -224$).

The selection of the ratio of integral to proportional gain (K_I/K_{PROP}) is based on the required rise time of $\frac{1}{4}$ -second. A parametric plot of the rise time versus K_{PROP} is given in Figure 4 for six values of K_I/K_{PROP} spaced uniformly from 1 to 251. The lower the ratio of K_I/K_{PROP} the higher the value of K_{PROP} is needed to meet the $\frac{1}{4}$ -second rise time. From Figure 4, a value of 100 for K_I/K_{PROP} yields the specified required rise time with $K_{PROP} > 35$, while a value of 50 for K_I/K_{PROP} requires a value of $K_{PROP} > 60$ to meet the specifications.

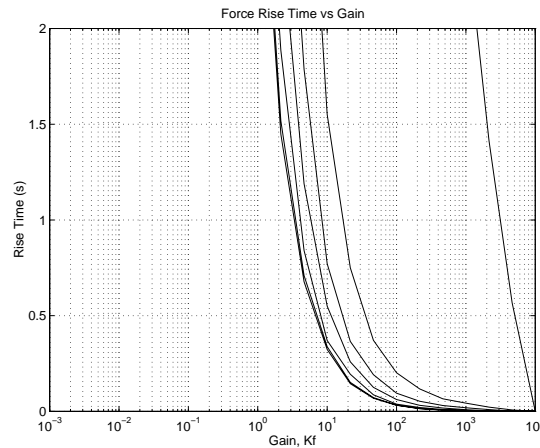


Figure 4. 95% Rise Time vs. K_{PROP} for Several Values of K_I/K_{PROP} .
 $(K_I/K_{PROP} = 1, 50, 100, 150, 200, 250$ from right to left)

Frequency domain analysis indicates larger the proportional gains yield the faster system response. However, PMAC is a digital position and force controller, and as such the force resolution and stability are directly affected by the proportional gain. Before the selection of the proportional and integral gains of the fixed-gain controller, a discrete design is examined.

Digital Controller Design

The force loop has a larger update time than the position loop, therefore a discrete model of the plant should be based on the combined continuous representation of the position loop and tool-workpiece stiffness. To obtain the discrete system the transfer function of the continuous system, it must be placed through a zero-order hold (ZOH) to transform it into the Z-domain.

The programmable controller updates each axis output voltage with a frequency of approximately 2,260 Hz; with a resulting sampling period measured at $T = 442.7 \mu\text{s}$. However, the outer force loop has longer calculations requiring 5 servo cycles of the position controller. Thus, the overall plant the servo update rate is 2.214-ms. The resulting discrete plant with the ZOH of equation is given in equations (6) and (7).

$$\frac{F(z)}{X_d(z)} = G_{PC}(z)G_{TWP}(z) = \frac{z-1}{z} Z \left\{ \mathcal{L}^{-1} \left[\frac{K_s 203}{s(s+224)} \right] \right\} \quad (6)$$

where $Z\{ \}$ represents the Z transform, yielding a discrete transfer function of

$$\frac{F(z)}{X_d(z)} = \frac{0.3543K_s}{(z-0.6091)} \quad (7)$$

The discrete PI-type controller for the force is described by equation (8).

$$G_{FC}(z) = K_{PROP} + \frac{K_I}{1-z^{-1}} = K_{PROP} \left(1 + \alpha \frac{z}{z-1} \right) \quad (8)$$

where

$$\alpha = \frac{K_I}{K_{PROP}}$$

The resulting discrete transfer function of the entire open-loop system is presented in equation (9).

$$G_{FC}(z)G_{PC}(z)G_{TWP}(z) = K_{PROP} \left(\frac{(1+\alpha)z-1}{z-1} \right) \left(\frac{0.3543K_s}{z-0.6091} \right) \quad (9)$$

In this relationship the overall gain of the transfer function is

$$K_F = 0.3543K_s K_{PROP} (1 + \alpha) \quad (10)$$

Using these relations a discrete root locus as a function of K_F is determined and presented in Figure 5, also illustrated with the unit circle for stability and showing lines of constant damping and natural frequency. Using these root locus data, Figure 6 plots the discrete root locus magnitude verses the proportional gain. Upon inspection of Figure 6, it can be seen that for

system stability the proportional gain must be less than 800. However, to provide a system response without overshoot it is desired to have all the discrete roots in the left-hand plane as close to the origin as possible (near Deadbeat control). This implies that the proportional gain must be less than 380. Since there is substantial process variability, it is desired to have the proportional gain smaller than this. Thus, a proportional gain in the range or 200-250 is selected for good system stability and reduced root sensitivity. The selected proportional gain value is divided by the constant coefficients given in equation (10) for implementation in the controller. It is interesting to note that the location of the plant zero (K_I/K_{PROP}) has little effect on selecting the limiting system proportional gain, as this is related to the location of the slower pole.

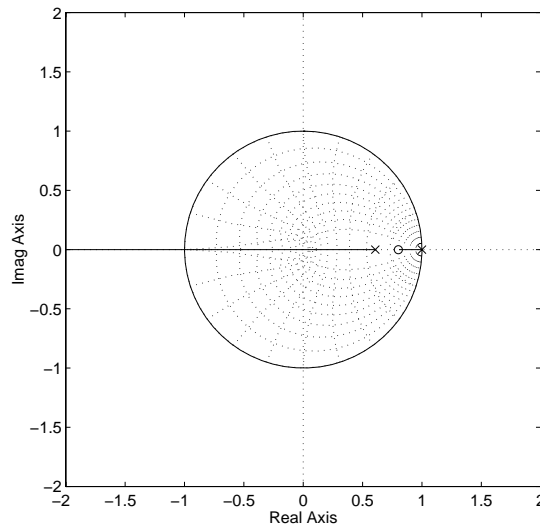


Figure 5. Discrete Root Locus for the Transfer Function of Equation (10) with $\alpha= 100$.

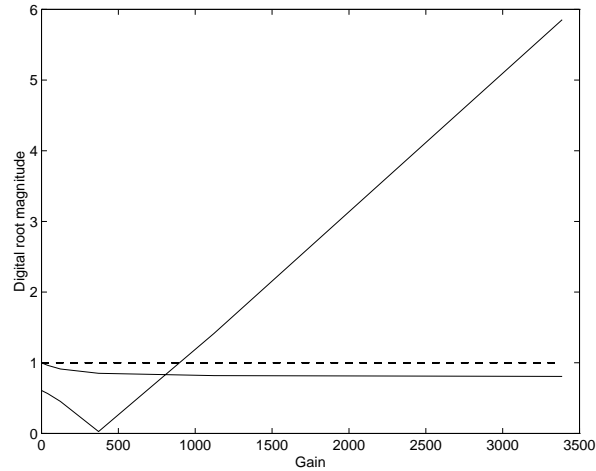


Figure 6. Discrete Root Magnitude vs. K_F with $\alpha= 100$.

With the fixed-gain controller designed and implemented, a set of experiments was conducted to verify the force response meets the desired control objectives and that saturation effects of the system have been sufficiently avoided. A step force input is commanded of the X-axis. It is servoed downward from the force error, with the tool end eventually making contact with the part and increasing the applied force to the desired set point. Figure 7 shows the resulting performance of the controller design using a proportional gain of 200 and an integral gain of 20,000 in terms of the output force for a commanded a step input of 25 N. It should be noted that the resolution of the encoder position is 2 μm which when multiplied by the spring constant yields a force resolution of 0.46 N. The specified rise time and limitations on force overshoot have been met for the fixed-gain controller, ignoring the process dynamics.

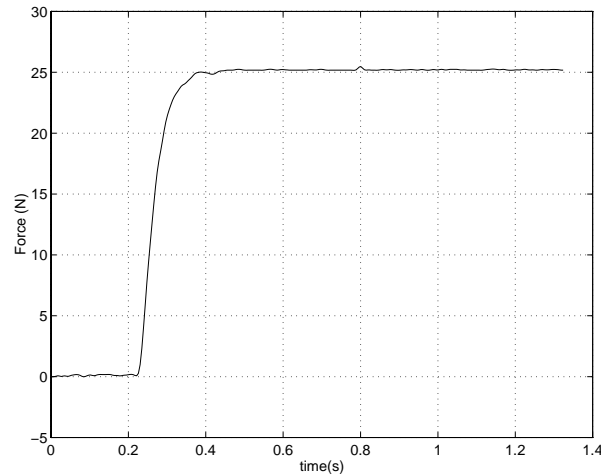


Figure 7. Fixed-Gain Force Controller Response to a 25-N Step Command.

ADAPTIVE PROCESS CONTROL

The grinding process has been modeled and has been shown to be a continuously, time-varying system (Part I). To better control the normal grinding force for the system, adaptive control methods are applied building on the successful real-time grinding model with on-line parameter estimation. The adaptive control strategy, process variation, and predictive power of the parametric model greatly influence the stability of the total system.

The approach taken in this adaptive force control effort for grinding is different from that of Tonshoff et al (1986). Tonshoff applied a fixed-gain controller to regulate the grinding force for an internal diameter grinder. Tonshoff used a separate off-line model estimation routine to determine the fixed-gains of the controller. In contrast the work undertaken here performs real-time estimation of the grinding process and uses a pole-zero cancellation approach to remove the process variation.

Adaptive Controller Development

The development of the adaptive force controller for the grinding process can proceed directly from the plant model of Part I, rewritten in equation (11).

$$G_{\text{TPW}}(s) = \frac{F_N(s)}{x_e(s)} = K_s \left(\frac{s}{s + \eta} \right) \quad (11)$$

where $\eta = K_p K_s V/A$. Combining equations (11) and (12) yield the following continuous plant transfer function.

$$G_{\text{PC}}(s)G_{\text{TWP}}(s) = \frac{F_N(s)}{x_d(s)} = 203K_s \left(\frac{s}{s + \eta} \right) \frac{1}{(s + 224)} \quad (12)$$

From the earlier work, it has been shown that $\eta \ll 224$. Thus, variations in the process can dominate the system response. A fixed-gain controller can lead to poor performance as well as instabilities. Thus, an adaptive controller is desired to mitigate the effects of changing process dynamics and maintain a high MRR and a stable controller. From equation (12) it can be seen that the process dynamics can be eliminated by a pole-zero cancellation using a PI-type controller. The controlled system would then be of the form

$$G_{\text{FC}}(s)G_{\text{PC}}(s)G_{\text{TWP}}(s) = \frac{F_N(s)}{E_F(s)} = 203K_s \left(\frac{s}{s + \eta} \right) \frac{K_{\text{PROP}}(s + \alpha)}{s(s + 224)} \quad (13)$$

In this scheme if the α (or K_I/K_{PROP}) of the PI controller in equation (13) is set to η , then the entire process grinding dynamics can be eliminated from the resulting equation. This reduces equation (13) to that of the previous situation of only a contact stiffness with a position loop, represented by equation (14).

$$G_{\text{FC}}(s)G_{\text{PC}}(s)G_{\text{TWP}}(s) = \frac{F_N(s)}{E_F(s)} = \frac{203K_s K_{\text{PROP}}}{(s + 224)} \quad (14)$$

where $\alpha = \eta$

But a discrete equivalent system is needed for the sampled plant in order to implement such a scheme on the PMAC controller. Again using the ZOH equivalent system a discrete plant is found.

$$\mathbf{G}_{\text{PC}}\mathbf{G}_{\text{TWP}}(z) = \frac{\mathbf{F}_N(z)}{\mathbf{X}_d(z)} = \left(\frac{z-1}{z}\right)Z\left[\mathcal{L}^{-1}\left[\frac{1}{s}203\mathbf{K}_s\left(\frac{s}{s+\eta}\right)\frac{1}{(s+224)}\right]\right] \quad (15)$$

$$\mathbf{G}_{\text{PC}}\mathbf{G}_{\text{TWP}}(z) = \frac{203\mathbf{K}_s}{224-\eta}\left(e^{-\eta T} - e^{-224T}\right)\left(\frac{z-1}{(z-e^{-\eta T})(z-e^{-224T})}\right) \quad (16)$$

denoting

$$\begin{aligned} C_o &= e^{-224T} \\ f_1(\eta) &= e^{-\eta T} \\ f_2(\eta) &= \frac{203\mathbf{K}_s}{224-\eta}(f_1(\eta) - C_o) \end{aligned} \quad (17)$$

Substituting (17), into (16) yields

$$\mathbf{G}_{\text{PC}}\mathbf{G}_{\text{TWP}}(z) = f_2(\eta)\left(\frac{z-1}{(z-f_1(\eta))(z-C_o)}\right) \quad (18)$$

The discrete PI-type controller can be rewritten as follows

$$\mathbf{G}_{\text{FC}}(z) = \frac{\mathbf{K}_{\text{PROP}}}{1+\alpha}\left(\frac{z - \frac{1}{(1+\alpha)}}{z-1}\right) \quad (19)$$

Thus if η varies sufficiently slowly or the controller is sufficiently fast, α can be chosen such that

$$\alpha = \frac{1}{f_1(\eta)} - 1 \quad (20)$$

then complete open-loop discrete transfer function is define as equation (21).

$$\mathbf{G}_{\text{FC}}\mathbf{G}_{\text{PC}}\mathbf{G}_{\text{TWP}}(z) = \frac{\mathbf{K}_{\text{PROP}}}{1+\alpha}f_2(\eta)\left(\frac{1}{z-C_o}\right) \quad (21)$$

Thus, the overall effective gain of the controller is

$$K_{\text{EFFECTIVE}} = \frac{K_{\text{PROP}}}{1 + \alpha} f_2(\eta) \quad (22)$$

Equations (17), (20), and (21) are used to determine the PI force controller gains in the controller design update of the self-tuning regulator. The effectiveness of the pole-zero cancellation is related to the process variation frequency spectrum and the gain update rate.

The implementation of this controller uses the windowed data handling scheme discussed in Part I. Thus, the size of the data window is the key parameter to the success of this approach. The smaller the window the faster the gain update. However, as the sample window gets smaller the variance of the parameter estimation increases. This reduces the confidence of the estimate and ultimately the reduces the probability of an effective pole-zero cancellation.

Stability

As the controller is stable by design for perfect estimation of the process parameters, the real plant stability is directly linked to the predictive power of the parameter estimation, the rate of parameter change, the controller update rate, and the update rate for the force controller gains. If the parameter prediction is perfectly accurate and the controller update is infinitely fast, then the stability is assured without a Lyapunov analysis. Thus, the stability of the adaptively controlled-force grinding system is linked to the variation in the model parameter(s) and the controller update rate.

A rigorous stability analysis in the sense of Lyapunov is complicated for STR systems, as the controllers are highly nonlinear. Indeed, the relationship of the regulated force to the estimated parameter can be quite convoluted and is difficult to attain in many instances. A more obvious and tangible evaluation of stability can be performed, for the STR problem at hand.

The first approach in answering the question of the stability for the adaptive force controlled grinding system is a parametric examination of the effect of poor estimation and adaptive performance. The effect of poor performance can be seen by examining the combined open-loop, discrete plant and controller transfer functions given in equations(19) and (21), combined to form equation (23)

$$G_{FC}G_{PC}G_{TWP}(z) = \frac{K_{PROP}f_2(\eta)}{1 + \alpha} \left(\frac{z - \frac{1}{1 + \alpha}}{(z - f_1(\eta))(z - C_o)} \right) \quad (23)$$

From equations (5-19) and (5-20) it can be seen that the poles of the open-loop system are all within the unit circle, so they are stable. The variable, α , is the ratio of the integral to the proportional gain; α is always a positive value. Therefore the transfer function zero is always positive and less than or equal to one (24).

$$z = \frac{1}{1 + \alpha} \quad (24)$$

Although an open-loop pole near unity is not desired in terms of the system performance specification, it is at worst marginally stable. Another possibility for instability is in the calculation of the proportional gain, given in equation (22). The overall gain is positive and is calculated in real-time to be stable dependent on the estimated grinding model. However, α is positive and determined by the controller. Thus even if the pole-zero cancellation is not accurate the effects do not cause the system to go unstable; however, performance may suffer.

RESULTS OF BENCHMARK FORCE REGULATION EXPERIMENTS

Two force regulation experiments (plunge and traverse grinding) were conducted to evaluate the effectiveness of the complete recursive estimation and adaptive control system. For comparison the previously designed fixed-gain controller is used to assess the improvements made by the adaptive controller.

Plunge Grinding Force Regulation

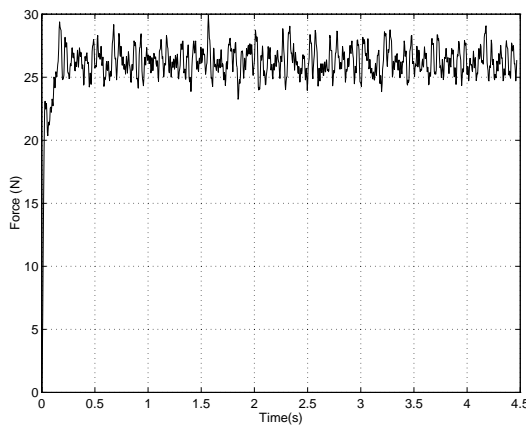
The first experiment is plunge grinding, with the grinder moving and force servoing in the feed direction. The accuracy and deviation of the regulated force is measured to assess any improvement. The force command input is 20 N with a step change to 25 N. This allows an assessment of the rise time for the step force change as well as determining the regulated force statistics.

Figure 8 plots a typical force regulation comparison. It is somewhat difficult to see the effect of the adaptive force regulation from the plots. The summary statistics for the all the specimens

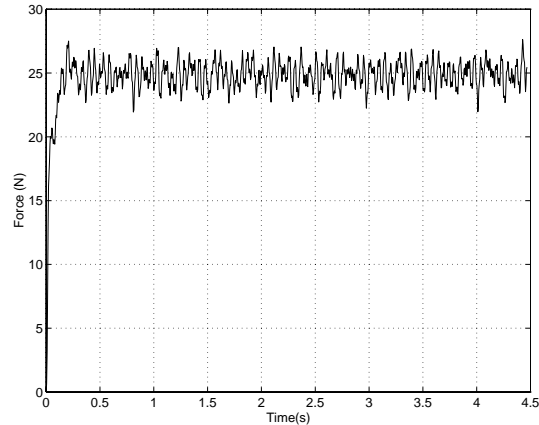
tested is given in Table 1. From these data the effects of the adaptive controller are more clear. The adaptive force regulation successfully reduces the standard deviation and range of the controlled normal force, albeit a small improvement. The adaptive controller also appears to have a mean normal force closer to the 25-N reference.

Table 1. Force Regulated Plunge Grinding Experimental Data Statistics.

Case	Material	Average Force (N)	Std. Dev. Force (N)	Max Force (N)	Min Force (N)	range Force (N)	Rise Time (sec)
Fixed Gain	4142	24.34	1.060	27.51	20.43	7.09	0.145
Adaptive	4142	25.18	0.962	27.88	21.67	6.21	0.133
Fixed Gain	A2	26.06	1.017	29.48	22.94	6.54	0.142
Adaptive	A2	24.78	0.975	27.48	21.94	5.54	0.142
Fixed Gain	O1	25.23	0.900	27.72	21.11	6.62	0.164
Adaptive	O1	25.52	0.800	27.66	22.41	5.25	0.149
Fixed Gain	8119	25.57	2.193	31.11	20.25	10.86	0.135
Adaptive	8119	25.92	1.979	30.97	21.17	9.80	0.124



(a) Fixed-Grain Force Control



(b) Adaptive Force Control

Figure 8. Plunge Grinding Force for AISI A2 Specimen.

Statistical Confidence of Force Control Plunge Grinding Results

The key measures of the step-force plunge grinding experiments to determine the benefit of the adaptive pole-zero cancellation are the mean, variance, and range of the measured normal force. While the mean value of the normal force is generally a good performance measure, the step

resolution of 2 μm and the effective stiffness of the axis and in-line strain-gage sensor (233 N/mm) limit the resolution of applied vertical normal force to 0.46 N. The force variance (the square of the standard deviation) and the force range are also good controller performance measures, and are calculated for each test by examining the 1,000 data points (4.5 s) collected.

To assess the effectiveness of the proposed adaptive pole-zero cancellation of the grinding process, it must be determined if the average improvements in the force mean, variance, and range are statistically significant. The answer lies in determining if the two data sets for the results of the fixed-gain controller and adaptive controller represent two separate populations with different means to some confidence level. This is accomplished by determining the confidence interval for the mean, \bar{x} , of each force experiment performance measure. The confidence interval for \bar{x} may be found by

$$\left[\bar{x} - t\left(\frac{\alpha}{2}; n-1\right) \frac{\sigma}{\sqrt{n}}, \quad \bar{x} + t\left(\frac{\alpha}{2}; n-1\right) \frac{\sigma}{\sqrt{n}} \right] \quad (25)$$

Here t is the Student-t distribution function, n is the number of samples, $(1-\alpha)$ is the confidence level, \bar{x} is the sample mean, and σ is the standard deviation of the data. Since the number of samples for each case is less than 30, a Student t-distribution is more appropriate than the normal distribution.

Applying equation (25) to the mean, standard deviation, maximum, minimum, and range the confidence interval of each is found.

It was found that the 90% confidence intervals do not overlap in comparing the average, standard deviation, maximum and minimum of the grinding normal force for adaptive and fixed-gain controllers for AISI-A2 and AISI-O1. The same is true for the AISI-4142 cases, expect for a small overlap for the standard deviation. In fact the average force shows no overlap with a 95% confidence for all these cases. This demonstrates a 90-95% confidence that the results represent two sample populations, and not simply chance sampling (indicating a statistically significant benefit from the adaptive controller).

For the AISI-8119 cases the results showed a slightly larger potential for overlap between the two sample populations of the adaptive and fixed-gain controller results. While for the AISI-8119 cases the standard deviation and minimum force values showed no overlap with a 95% confidence, the mean force showed no overlap only to an 80% confidence level. Thus the confidence in the benefits of the adaptive controller performance for the 8119 steel is 80-95%.

Traverse Grinding Force Regulation

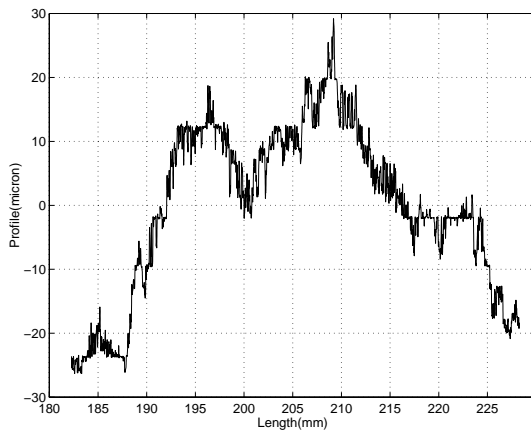
The second benchmark experiment is a traverse grind over a flat surface. Here the results of force regulation should provide better repeatability of the surface profile after grinding. This is an example of fine finishing. A flat ground surface is used to simplify the determination of the real-time material removal.

Note an LVDT was used for profile measurement, and acts as a low-pass spatial filter on the surface. Although very fine resolution measurements (such as from a profilometer) were not obtained, the measurements are a good indicator of the surface following capability of the force controllers. Three scans are made along the traverse grinding directions for each grind. The scans are spaced equally across the 10 mm width of the specimens. Data are recorded at approximately every 4 μm along the specimen. The LVDT resolution is under 0.1 μm .

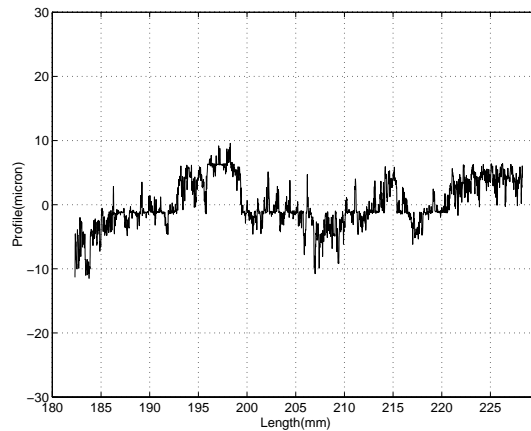
The summary profile statistics for all the specimens tested is given in Table 2. The statistics for the three scans (per ground surface) are then averaged to obtain the values in Table 2. The adaptive controller provides a better surface profile following capability from these data. Plots of the profile data for the AISI O1 material are given in Figure 9 for the fixed-gain controller and the adaptive controller. The adaptive controller yields visually smaller surface deviations although, the improvements appear to decline somewhat with the material hardness. The small, sharp displacements are attributed to stiction in the LVDT core and to electro-magnetic noise.

Table 2. Traverse Grind Surface Profile Statistics.

Material	O1	A2	4142
	units: (mm)		
<u>Adaptive Control</u>			
Absolute Mean	3.66	4.81	8.00
RMS mean	4.57	5.92	9.46
Range	27.57	32.77	44.75
Std. Deviation	4.57	5.93	9.46
<u>Fixed-Gain Control</u>			
Absolute Mean	10.26	12.88	11.40
RMS mean	12.56	14.49	14.21
Range	58.53	59.89	65.54
Std. Deviation	12.57	14.49	14.21
<u>Ratio AC/FG</u>			
Absolute Mean	35.7%	37.3%	70.2%
RMS mean	36.4%	40.9%	66.6%
Range	47.1%	54.7%	68.3%
Std. Deviation	36.4%	40.9%	66.6%



(a) Fixed-Gain Force Control



(b) Adaptive Force Control

Figure 9. Traverse Grinding Surface Profile for AISI O1 Specimen.

Thus the adaptive control and estimation technique appears to provide an improvement in surface following for fine finishing. Although these improvements appear to decline somewhat with the material hardness. This is expected from the model form. For harder materials with low material removal rates the process impedance is larger, with less benefit from process cancellation through the controller. In this situation the tool compliance may be the most significant

impedance component. However, it is evident that for very high stiffness industrial grinders the process impedance will be dominant.

These results agree well with the present literature. It should also be noted that several important findings were obtained from the work of Hahn and Lindsay. They showed a correlation to increases in force to poorer surface finish. This supports the conclusion that higher fidelity force regulation will provide better surface following.

CONCLUSION SUMMARY

Several important observations have been made. The model of equation 4-1 has been successfully applied to several materials. These experiments have also yielded some material

The resulting adaptive control and estimation system has been shown to improve the fidelity and stability of force regulation in plunge grinding, as compared to fixed-gain controllers. This is proved by the results of the benchmark experiments. The adaptive (pole-zero cancellation) controller has been shown to be effective in mitigating the effects of the grinding process. A higher fidelity force regulator with greater stability has been developed for plunge grinding. Similarly in traverse grinding, the surface profile following capability improves with the adaptive pole-zero cancellation technique, as contrasted to the fixed-gain controller. The final implementation of the adaptive controller and estimator yielded a superior grinding force controller.

RECOMMENDATIONS

There are several areas for future work, building on this research. The first of which is the development of heavy industrial grinding applications of this approach. Specifically, cylindrical grinding can benefit from the techniques developed in this research. The methodology of this work may be applied to the develop process knowledge and control for other multi-contact fine finishing processes such as honing and polishing. The improved surface profiles obtained from fine-finishing experiments merit the continued grinding research to relate surface finish to real-time grinding process parameters.

Surface finish research would be best performed on more rigid industrial grinders, than on the test fixtures of this research. The unmodeled dynamics of the grinder contribute to the estimation of K_p . The use of less compliant (production scale) equipment should eliminate much of these effects. The “true” process dynamics of K_p could be more thoroughly investigated.

Additions to the implemented grinding force controller approach might include, a force trajectory planner for providing constant material removal on a non-planar geometry. Extending this work

to three dimensional surface grinding would require significant effort to include a geometric model of the part or to include surface preview for determining material removal. Inclusion of real-time wheel wear measurements into a grinding model would also be worthy of future investigation. Application of piezoelectric, fast tool servos for high frequency control and compensation may provide reduction of the effects of system vibrations, allowing for the use of more flexible inexpensive grinders. This capability would also allow for higher precision not found in current 3-D grinding systems.

BIBLIOGRAPHY

- Astrom, K. J. and Wittenmark, B., *Adaptive Control*, Addison-Wesley Publishing Co., Reading MA, 1989.
- Franklin, G. F., Powell, J. D., and Workman, M. L., *Digital Control of Dynamic Systems*, Addison-Wesley, Reading, MA, Second Edition, 1990.
- Fussell, B. K., Srinivasan, K., "Model Reference Adaptive Control of Force in End Milling Operations," *1988 American Control Conference*, Vol. 2, pp. 1189-94.
- Hahn, R. S. and Lindsay, R. P. "Principles of Grinding Part I Basic Relationships in Precision Machining," *Machinery*, July 1971, pp. 55-62.
- Hahn, R. S. and Lindsay, R. P. "Principles of Grinding Part II The Metal Removal Parameter," *Machinery*, August 1971, pp. 33-39.
- Landau, I. D., *Adaptive Control*, Dekker, New York, 1979.
- Kurfess, T.R., Nagaruka, M.L., "A Geometric Representation of Root Sensitivity," *ASME Journal of Dynamic Systems, Measurement, and Control*, 1994, Vol. 116, No. 4, pp. 305-309.
- Kolarits, F. M., "Dynamic Modeling Of End Milling Forces and Surface Geometry and Adaptive Pole Placement Force Control," Rensselaer Polytechnic Institute, Ph.D. Thesis, 1990.
- Tonshoff, H. K., Zinngrebe, M., Kemmerling, M., "Optimization of Internal Grinding by Microcomputer-Based Force Control," *Annals of the CIRP*, Vol. 35, No. 1, 1986. pp. 293-296.